Development of Neutral Molecular Beam Injector for Two-Dimensional Edge Density Measurement

H. TSUCHIYA, T. MORISAKI[1)], A. KOMORI[1)], Y. TAKAHASHI[2)], K. TOI[1)], H. ZUSHI[3)], O. MOTOJIMA[1)] and LHD Experimental Group[1)]

Graduate University for Advanced Studies, Toki 509-5292, Japan
[1)]*National Institute for Fusion Science, Toki 509-5292, Japan*
[2)]*Department of Energy Engineering and Science, Nagoya University, Nagoya 464-8603, Japan*
[3)]*Research Institute for Applied Mechanics, Kyushu University, Kasuga 816-8580, Japan*

(Received 6 January 2007 / Accepted 26 April 2007)

A sheet-shaped thermal lithium beam probe has been developed for two-dimensional density measurements in the edge region of the torus plasma. For the production of an intense and uniform beam, the optimization of the nozzle shape and slit width of the beam injector has been performed. Beam density profiles at the observing region in the plasma were estimated with numerical calculations using a Monte Carlo technique for several kinds of nozzles and combinations with slits. Experiments on the test stand were also carried out, and pretty good agreement was found between numerical and experimental results. Based on these examination and optimization for the nozzle and slits, we have constructed a sheet-shaped beam injector for the large helical device. In spite of the long distance (about 3 m) from the injector, it is estimated that the thickness of the sheet-shaped beam is ~90 mm (full width at half maximum).

Keywords: thermal lithium beam probe, LHD, sheet-shaped beam, neutral molecular beam injector, Mote Carlo technique, 2D measurements, edge plasma

DOI: 10.1585/pfr.2.S1096

1. Introduction

The study of particle and energy transport in the fusion edge plasma is crucial, since it defines the boundary condition of the core plasma and may affect the formation of the edge pedestal or edge transport barrier. In addition to the fluctuation induced cross-field transport, edge localized modes (ELMs) or blobs [1–4] are also excited in this region, which have a considerable portion of heat load and particle flux to the vessel wall. From the view point of the issues related to the plasma facing components (PFCs), it is favorable if the particle and energy influx to PFCs can be controlled, based on the accumulation of the knowledge about the edge transport.

Recently it has been known that ELMs and blobs do not always appear symmetrically in toroidal and/or poloidal directions, even in tokamaks with the axisymmetric configuration. Especially in helical devices, the edge magnetic configuration is intrinsically three-dimensional thus its structure is highly complicated. In view of such conditions, the one-point or one-dimensional (1D) measurement by using e.g., a conventional Langmuir probe with an extremely small observation area is not sufficient to know the overall picture of the phenomena. In order to get rid of this disadvantage, the two-dimensional (2D) measurement with a thermal lithium beam probe (LiBP) has been developed in the Compact Helical System (CHS) and the Large Helical Device (LHD) in National Institute for Fusion Science. The 2D-LiBP in CHS [5] actually produces 2D density profiles; however, it is essentially a 1D system, i.e., a 2D profile can be reconstructed by scanning a pencil beam shot by shot. Therefore it has no time resolution in a 2D reconstructed profile, and cannot deal with transient phenomena two-dimensionally. On the other hand, the 2D-LiBP by use of the sheet-shaped beam developed in LHD [6–8] is suitable for the two-dimensional measurement. With the combination of the sheet-shaped beam and the 2D optical detector, it is possible to detect fast and transient phenomena two-dimensionally, to say nothing of 2D density profiles.

For the precise measurement, the intense, uniform and thin beam is necessary to achieve good time and spatial resolutions. In this paper, evaluation of the sheet-shaped beam produced with various types of nozzles is presented. The optimization of nozzles and slits was mainly carried out by numerical simulations. Comparison test between the simulation and the experiment are also presented. Brief introduction of 2D-LiBP is shown in section 2. The optimization process and evaluation of the sheet-shaped beam for the 2D measurement is described in section 3. After describing the comparison between simulation and experiment in section 4, the setup for LHD and the beam performance expected by the calculation are presented in section 5. Finally summary is given in section 6.

author's e-mail: tsuchiya.hayato@lhd.nifs.ac.jp

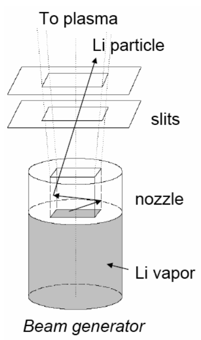

Fig. 1 Schematic of sheet-shaped beam production.

2. General Description of 2D Thermal LiBP

The 2D-LiBP is a kind of a beam probe which utilizes sheet-shaped 2D neutral lithium beam. Lithium atoms vaporized in an oven at ~ 800 K are conducted to the plasma through three slots which shape the beam into a sheet. By injecting the sheet beam into the plasma, a 2D density profile, e.g. at the poloidal cross section, is cut out from the plasma column. Lithium atoms in the plasma emit photons by electron impact excitation. The rate of local photon emission $I(r)$ at the position r for the lithium resonance line Li I (670.8 nm) is given by

$$I(r) = n_e(r) n_{Li}(r) \langle \sigma v \rangle_e V \Omega / 4\pi \quad (1)$$

where $n_e(r)$ is the local electron density, $n_{Li}(r)$ the local beam density, $\langle \sigma v \rangle_e$ the rate coefficient for 2^2S-2^2P electron impact excitation, V the observation volume, and Ω the solid angle determined by an optical detection system. The $\langle \sigma v \rangle_e$ is assumed to be constant in our analysis because it is almost constant within the range of factor 2 among 10-100 eV [9].

A 2D image of Li I emission from the plasma is detected two-dimensionally by CCD or photomultiplier tube (PMT) array with an interference filter of Li I line. From the image, 2D density profiles can be reconstructed [8] and characteristics of the fluctuation, e.g. amplitude, spectra, propagation, etc. can also be extracted.

3. Optimization of 2D Beam Injector

3.1 Numerical calculation

Figure 1 shows a schematic of the 2D beam injector. As indicated by arrows, lithium atoms pass through the nozzle of the oven, reflecting at the wall of the nozzle. Some atoms, of course, can pass through the nozzle without any reflection. The lithium beam coming out from the nozzle flies to the slit which trims off the edge of the beam, i.e. excess lithium atoms are intercepted. After passing through some slits, the beam is shaped to be sheet.

Trajectories of lithium atoms from oven to the plasma are numerically simulated using the Mote Carlo technique to optimize the beam injector for the effective injection. In the calculation a source of the lithium atoms is located at the bottom of the nozzle, and atoms are launched in arbitrary directions according to the Monte Carlo manner. Atoms striking the nozzle wall are all reflected in arbitrary directions. No atom is trapped at the nozzle wall, since its surface is hot enough to vaporize it again. Collisions between atoms are not taken into account because the beam density is not so high. This calculation process for an atom, i.e. free flight and reflection at the nozzle wall, is continued until it reaches the target plasma after passing through the final slit or it returns to the bottom of the nozzle (source position) again. The trajectory tracing for an atom is terminated when the atom is intercepted by the slit. By measuring the number of atoms at the target plasma, we can estimate the beam flux and its profile to be injected to the plasma.

Table 1 Performance and characteristics of 2D beams produced with various types of nozzles.

	Type-1	Type-2	Type-3	Type-4
nozzle	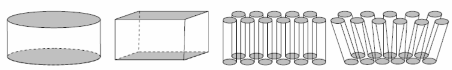			
	Φ25mm	25mm × 5mm	Φ3mm × 11	Φ3mm × 11
Area of nozzle	490.9mm²	125mm²	77.8mm²	77.8mm²
$\Gamma_{ex} / \Gamma_{en}$	47.7%	31.8%	14.5%	14.5%
$\Gamma_{sl} / \Gamma_{en}$	4.23%	1.63%	0.32%	0.32%
$\Gamma_{pl} / \Gamma_{en}$	0.016%	0.024%	0.022%	0.017%
FWHM at plasma	240.0mm	43.75mm	38.5mm	37.4mm
α : exponent of attenuation $\Gamma(z) = \Gamma_{en} z^{-\alpha}$	2.43	2.12	1.88	1.92

First, the effect of nozzle shape is investigated in four different types of nozzle, as shown in Table 1. The type-1 and type-2 are the single-hole nozzles. On the other hand, the type-3 and type-4 are multi-hole nozzles which consist of 11 small apertures whose diameter is 3 mm, expecting better collimation. Holes of the type-4 nozzle are fanned out to spread the beam rapidly. The length of all nozzles is 20 mm. Generally speaking, for the type-3 and type-4 nozzles, the longer and narrower hole has better collimation performance. However it is limited, by the technical reason, to 20 mm in length and 3 mm in diameter, respectively. In the calculation, a slit with a rectangular aperture of 35 mm × 6 mm is set 53 mm apart from the nozzle. The 1×10^7 lithium atoms were launched into the nozzle in arbitrary directions. Particle fluxes at the exit of the nozzle Γ_{ex}, slit Γ_{sl} and plasma Γ_{pl} were calculated, and their ratio to the flux at the entrance of the nozzle Γ_{en} are presented in Table 1. It is found that the type-2 or type-3 slit has the highest $\Gamma_{pl} / \Gamma_{en}$, i.e. highest beam density at the plasma to be observed.

Another important factor of the beam performance is its divergence after it passes through the nozzle. If the beam divergence is large, most of beam particles (Li atoms) cannot pass through the final slit. In other words, most of particles are intercepted by the slits, which are consequently piled up around the slits. This is an undesirable situation because a stack of Li often troubles the instrument. Furthermore this low efficiency in the beam production means the superfluous consumption of Li. Thus the beam with small divergence is favorable. In order to estimate the beam divergence, the attenuation of the beam flux from the exit of the nozzle was calculated. The results are also presented in Table-1 with an index of α where α is an exponent defined by,

$$\Gamma(Z) = \Gamma_{\mathrm{ex}} Z^{-\alpha} \quad (2)$$

In Eq. (2), Z is a distance from the exit of the nozzle along the beam. If the beam source is a point source on a plane and it is entirely isotropic, α should be ~ 2. It is found that α is larger than 2 in the case of single-hole nozzles, i.e. type-1 and type-2. This can be explained that quite a few particles pass through the hole diagonally without any collision with the wall of the hole, hence the beam diverges from the exit of the nozzle. On the other hand, α of multi-hole nozzles (type-3 and type-4) is less than 2, which indicates that the beam is well collimated by the hole. This is due to the decrease of particles which pass through the hole obliquely without any collision to the wall.

The width of the sheet beam is also important because it affects the spatial resolution. If the beam is relatively thick, emissions in the sheet are integrated along the line of sight. The thin beam can cut out the thin observing plane from the plasma column. For the estimation of the beam width, the full width at half maximum (FWHM) at the observing region was calculated, and the results are shown in Table 1. It can be known that multi-hole type nozzles are also better than single-hole nozzles.

In conclusion, we have decided to use the type-3 multi-hole nozzle for the 2D LiBP in LHD. The distance from the nozzle to the plasma is so long (more than 3 m) in LHD that the fanned nozzle (type-4) is not necessary.

3.2 Experiment

In order to examine the accuracy of the calculation mentioned in section 3.1, measurements of the beam performance with a type-4 nozzle were experimentally carried out. The sheet beam injector was installed in the test chamber. For the measurement of the beam flux, a quartz micro balance which could be scanned in two directions (R, Φ; see Fig. 2) across the beam was employed. With this detector, flux profiles of the sheet beam can be obtained. Flux profiles can also be seen directly, if a viewing window is installed, instead of the detector. In this setup, a thin lithium film deposited on the window surface can be seen, as shown in Fig. 2.

In Fig. 3, the numerical and experimental results are compared. Figure 3 (a) and (b) show the flux profiles along R and Φ axes which are depicted in Fig. 2, supposing the major radius and toroidal directions, respectively. It can clearly be seen that numerical (solid lines) and experimental (closed circles) results agree well, except for a few points in the central region in Fig. 3 (a). This result encourages us to use our simulation code for the optimization of the beam injector in actual experimental devices.

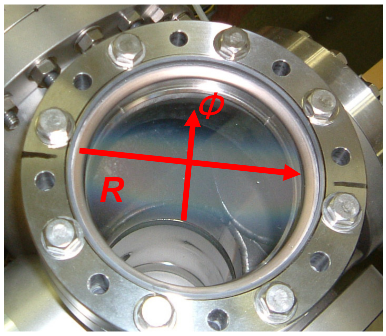

Fig. 2 Picture of the deposited lithium film on window surface.

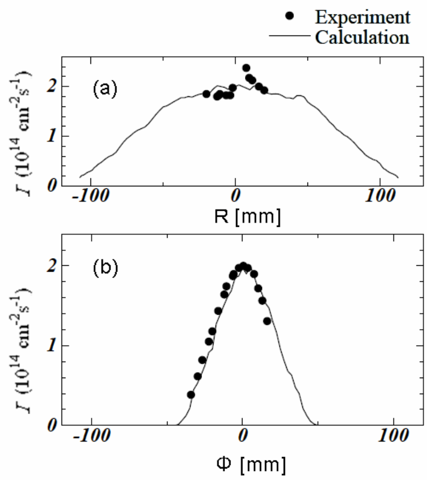

Fig. 3 Comparison between numerically (line) and experimentally (dots) obtained beam flux profiles. Picture of the deposited lithium film on window surface.

4. Installation in LHD

Based on the optimization process described in previous section, the sheet beam injector with the type-3 nozzle was installed in LHD to realize the 2D edge plasma measurements. The beam is injected into the LHD plasma from the lower port through 3 independent slits, as shown in Fig. 4. The schematic of the nozzle and three slits are shown in Fig. 1. Note that the three slits are behind the gate valve, i.e. in the port. The direction of the sheet surface was set to cut the poloidal plane, i.e. normal to the sheet faces the toroidal direction Φ (see Fig. 2 and Fig. 4). The expected beam flux profiles at the observing volume ($Z = -1$ m) are presented in Fig. 6, where $Z = 0$ is on the midplane. In the calculation actual dimensions were used for the parameters related to the apparatus. From Fig. 6, it

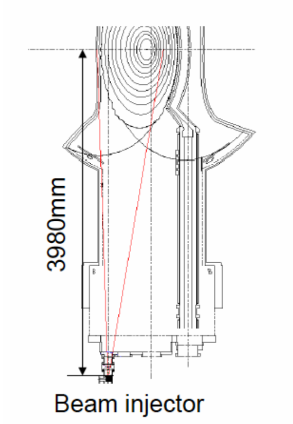

Fig. 4 Schematic of 2D measurement in LHD

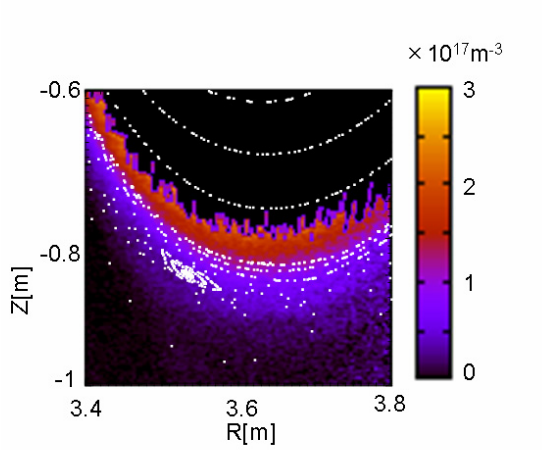

Fig. 5 Reconstructed 2D edge electron density profile in LHD.

can be seen that the radial (*R* direction) uniformity of the sheet beam is about ± 50 % and the thickness of the sheet beam (*Φ* direction) is ~ 9 cm (FWHM).

The 2D edge density measurement was tried during the electron cyclotron resonance heating discharge [6]. Figure 5 shows a 2D electron density profile reconstructed from the Li I emission distribution on the sheet beam. The 2D emission signal was detected with a CCD camera installed in the horizontal port. The calculated closed magnetic surfaces and open ergodic region depicted with contours and scattered dots, respectively, are superimposed on the density profile. In this discharge, the beam could penetrate into the core region through the last close flux surface (LCFS), since the line averaged density was relatively low ($\sim 2.0 \times 10^{17}\,\mathrm{m}^{-3}$). It is found that the 2D electron density profile agrees well to the calculated magnetic surfaces, i.e. the electron density rapidly increases from the LCFS, having a finite density gradient. On the other hand, it can be seen that the low density plasma spreads over the ergodic region across the LCFS.

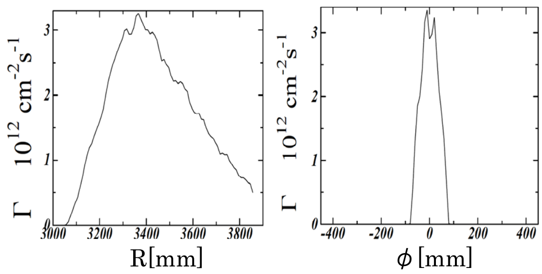

Fig. 6 Expected beam flux profiles at the observing region in LHD.

5. Summary

For the estimation of the beam performance of 2D LiBP, we have developed a particle tracing code using the Monte Carlo technique. The calculated beam flux was compared with experimentally measured one. Both results were found to agree well.

In the optimization process of the 2D beam injector using the numerical calculation code, we have reached a conclusion that a multi-hole type nozzle is better than a single-hole type nozzle to produce an intense and efficient sheet beam. Based on these results, we constructed the 2D LiBP system and installed it in LHD. In the preliminary experiment, 2D electron density profiles has been measured successfully. It is found that the measured profile indicates the edge magnetic configuration.

Acknowledgments

The authors would like to thank Prof. S. Takamura and Prof N. Ohno for many useful discussions and Mr. Y. Inada for his help in the experiment. This work is supported by NIFS under Grant (No. NIFS06ULPP507) and by the Grant-Aid for Scientific Research from MEXT of the Japanese government.

[1] S.I. Krasheninnikov, Phys. Rev. Lett. **A 283**, 368 (2001).
[2] J.A. Boedo *et al.*, Phys. Plasmas **8**, 4826 (2001).
[3] D.A. D'Ippolito *et al.*, Phys. Plasma **10**,4029 (2003).
[4] D.A. Russell *et al.*, Phys. Rev. Lett. **93**, 265001 (2004).
[5] K. Nakamura *et al.*, Rev. Sci. Instrum. **76**, 013504(2005).
[6] Y. Takahasi *et al.*, J. Plasma Fusion Res. **1**, 103 (2006).
[7] Y. Takahashi *et al.*, J. Korean Phys. Soc. **49**, S175 (2006).
[8] H. Tsuchiya *et al.*, Rev. Sci. Instrum. **77**, 10F526 (2006).
[9] T. Morisaki *et al.*, Rev. Sci. Instrum. **74**, 1865 (2003).